European Journal of Medicinal Chemistry 44 (2009) 4259–4265

Contents lists available at ScienceDirect

European Journal of Medicinal Chemistry

journal homepage: http://www.elsevier.com/locate/ejmech

Original article

Pharmacophore modeling and virtual screening for the discovery of new transforming growth factor-β type I receptor (ALK5) inhibitors

Ji-Xia Ren, Lin-Li Li, Jun Zou, Li Yang, Jin-Liang Yang, Sheng-Yong Yang*

State Key Laboratory of Biotherapy and Cancer Center, West China Hospital, West China Medical School, Sichuan University, Chengdu 610041, China

ARTICLE INFO

Article history:
Received 3 December 2008
Received in revised form
18 May 2009
Accepted 9 July 2009
Available online 16 July 2009

Keywords:
Transforming growth factor-β type I receptor
Pharmacophore modeling
Kinase inhibitor
Virtual screening
Catalyst

ABSTRACT

Inhibitors of transforming growth factor-β Type I Receptor (ALK5) have been thought as potential drugs for the treatment of fibrosis and cancer and a considerable number of ALK5 inhibitors have been reported recently. In order to clarify the essential structure–activity relationship for the known ALK5 inhibitors as well as identify new lead compounds against ALK5, 3D pharmacophore models have been established based on the known ALK5 inhibitors. The best pharmacophore model, Hypo1, was used as a 3D search query to perform a virtual screening. The hit compounds were subsequently subjected to filtering by Lipinski's rule of five and docking studies to refine the retrieved hits. Finally a total of 100 compounds were obtained and some of them were selected for further *in vitro* and *in vivo* assay studies.

1. Introduction

The transforming growth factor-β (TGFβ) signaling plays critical roles in the regulation of a variety of physiological processes including cell growth, differentiation, development, and immune response [1–3]. The TGFβ signaling pathway is initiated through the binding of mature TGFβ to transmembrane TGFβ type II receptor (TβR-II), followed by the recruitment of type I receptor (TβR-I/ALK5) and subsequently the activation of TβR-I by TβR-II. The activated ALK5 then phosphorylates the major downstream signaling molecules Smad2 and Smad3 proteins, which then form a complex with Smad4. This complex translocates into nucleus and regulates the transcription of specific genes [4,5].

Dysregulation of the TGFβ signaling might lead to some pathological changes. For example, many studies have shown that TGFβ is the main cytokine driving fibrosis associated with chronic inflammation in disease states such as liver fibrogenesis, pulmonary fibrosis, and chronic glomerulonephritis [6–9]. In addition, TGFβ has also been demonstrated to be involved in tumor progression and some autoimmune diseases [10–13]. Blocking TGFβ signaling is thought to be a promising approach to the treatment of these kinds of pathological conditions [5,8,14]. As TβR-I is the key molecule within the TGFβ signaling pathway, it has been believed as a critical target for the blockage of TGFβ signaling [15,16]. Indeed, functional inhibition of TβR-I has been shown to be able to suppress the fibrosis and cancer in animal models [17–19].

Currently, many pharmaceutical companies including GlaxoSmith-Kline, Scios, Pfizer, Biogen and Lilly, as well as lots of academic institutions have been involved in the development of small molecule inhibitors of ALK5 [20]. As far as we know, more than one hundred small molecule inhibitors against ALK5 have been reported publicly at present. These provide a solid basis for elucidating the quantitative structure–activity relationship (QSAR) of these diverse compounds, and further identifying new ALK5 inhibitors.

In the present study, we firstly collected all the ALK5 inhibitors from different public resources including patents and journals [17,21–30]. Based on these collected ALK5 inhibitors, we developed both qualitative and quantitative pharmacophore models whose purpose is to identify the critical pharmacophore features necessary for potent ALK5 inhibitors as well as clarify the quantitative structure–activity relationship for the known ALK5 inhibitors. Then the best quantitative model was used as 3D search queries for chemical databases, including Specs, NCI, MayBridge and Chinese Nature Product Database (CNPD) to identify new inhibitors of ALK5. The hit compounds were subsequently subjected to filtering by Lipinski's rule of five [31] and docking studies to refine the retrieved hits. It was expected that these established models should

* Corresponding author. Tel.: +86 28 85164063; fax: +86 28 85164060.
E-mail address: yangsy@scu.edu.cn (S.-Y. Yang).

0223-5234/$ – see front matter © 2009 Elsevier Masson SAS. All rights reserved.
doi:10.1016/j.ejmech.2009.07.008

be capable of correctly reflecting the structure–activity relationship of ALK5 kinase inhibitors, as a result, be helpful to the identification of novel ALK5 inhibitors. Previously, Singh et al. [32] have established a qualitative pharmacophore model based on a known ALK5 inhibitor (SB203580) and performed a shape-based virtual screening. However, as far as we know, our work is the first report on the quantitative pharmacophore/QSAR modeling of ALK5 inhibitors.

2. Results

2.1. Pharmacophore modeling

Before the start of pharmacophore modeling, we collected a total of 106 ALK5 inhibitors from different literature resources [17,21–30], from which, 21 compounds were carefully chosen to form a training set, which was based on the principles of structural diversity and wide coverage of activity range (here the IC_{50} values of the training set compounds span a range of four orders of magnitude: ranging from 4 nM to 30 000 nM). Structures and biological activities of the training set compounds are shown in Fig. 1. The remaining compounds were used as a test set (see Table S1 in Supplementary material).

Firstly, qualitative HipHop models were generated based on the five most-active compounds in the training set (**1**–**5**), whose purpose is to identify the critical common chemical features necessary for potent compounds and hence to provide some information for the quantitative pharmacophore modeling [33]. The most-active compound **1** was considered as 'reference compound' specifying a 'principal' value of 2 and a 'MaxOmitFeat' value of 0. The 'principal' and 'MaxOmitFeat' values were set to 1 for the remaining 4 compounds. The best HipHop hypothesis, shown in Fig. 2A, contains six features: one hydrogen-bond acceptor (A), one hydrogen-bond donor (D), one hydrophobic aliphatic moiety (L), one hydrophobic aromatic feature (Z), and one ring aromatic feature (R), implying that these features are necessary and important for a potent ALK5 inhibitor. Fig. 2B presents the mapping of the best HipHop pharmacophore model onto the most-active compound **1** (IC_{50}: 4 nM) in the training set.

Following the information provided by the HipHop model, hydrogen-bond acceptor (A), hydrogen-bond donor (D), hydrophobic aliphatic moiety (L), hydrophobic aromatic feature (Z), and ring aromatic feature (R) were chosen as the initial chemical features in the quantitative pharmacophore modeling. To consider the steric effect, the value for "excluded volume" was set to 2. The carefully selected 21 compounds (**1**–**21**, Fig. 1) were used as the training set compounds in the HypoRefine run. The top 10 hypotheses and the results of statistical parameters are given in Table 1. The best hypothesis Hypo1, shown in Fig. 3A, is characterized by the lowest total cost value (92.055), the highest cost difference (107.807), the lowest RMSD (1.197), and the best correlation coefficient (0.944651). The fixed cost and null cost are 75.6445 and 199.862 bits, respectively. Hypo1 contains four features: one hydrogen-bond acceptor, one hydrogen-bond donor,

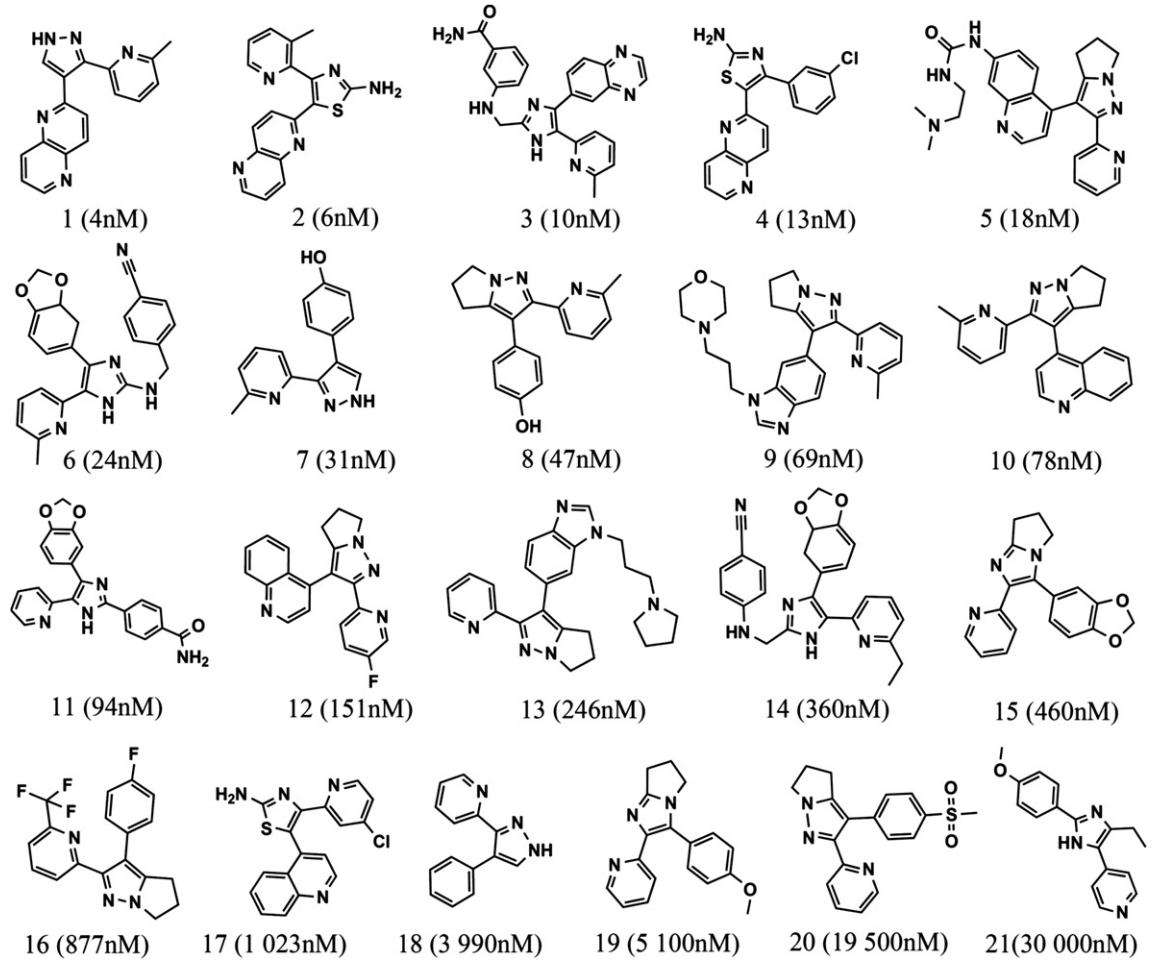

Fig. 1. Chemical structures of ALK5 kinase inhibitors in the training set together with their biological activity data (IC_{50} values, nM) for HypoRefine run.

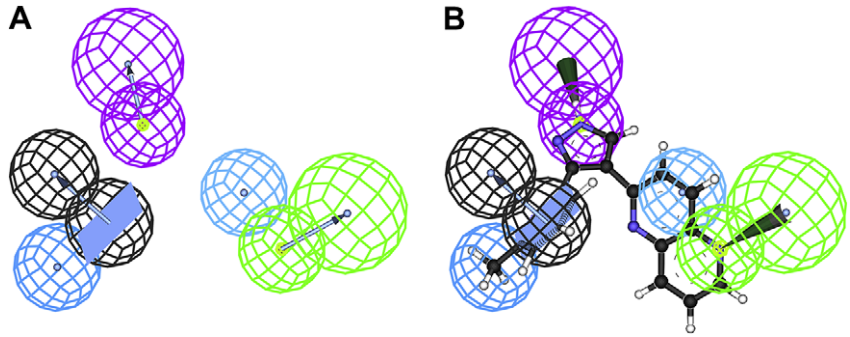

Fig. 2. Pharmacophore model of ALK5 inhibitors generated by HipHop. (A) The best ranking HipHop model. (B) HipHop model aligned with the most-active compound **1** (IC_{50}: 4 nM). These features are color coded: green – hydrogen-bond acceptor, magenta – hydrogen-bond donor, blue – hydrophobic aromatic feature, dark blue –hydrophobic aliphatic moiety, black – aromatic ring feature. (For interpretation of the references to color in this figure legend, the reader is referred to the web version of this article.)

and two hydrophobic aromatic features. Two excluded volumes are also involved in Hypo1. The 3D space and distance constraints of these pharmacophore features are shown in Fig. 3B.

Then Hypo1 was used to estimate the inhibitory activities of the 21 training set compounds. Table 2 shows the estimated and experimental inhibitory activities (IC_{50}) of the 21 training set molecules. Clearly the IC_{50} values of the training set compounds were correctly predicted, indicating that Hypo1 is a good pharmacophore model. Fig. 3C and D present the Hypo1 aligned with the most-active compound **1** (IC_{50}: 4 nM) and the least active compound **21** (IC_{50}: 30 000 nM) in the training set. Clearly, all hypothesis features are mapped very well with the corresponding chemical functional groups on compound **1**, while two hypothesis features, i.e. one hydrogen-bond donor and one hydrophobic aromatic feature, are not mapped with any functional group on compound **21**. These reflect the validity of the pharmacophore model Hypo1 to some extent.

2.2. Validation of the pharmacophore model

2.2.1. Test set method

The test set method is for examining whether the pharmacophore model is capable of predicting the activities of external compounds of the test set series. The test set contains 85 compounds structurally different from the training set molecules. All the test set molecules were prepared by the same way as that for the training set molecules. Hypo1 was regressed against the 85 test set compounds which gave a correlation coefficient of 0.841 between experimental and estimated activities. The results are presented in Fig. 4. Obviously, Hypo1 has a good ability to predict the activities of a wide variety of ALK5 inhibitors (the detailed information is provided in Supplementary material, see Table S2).

Table 1
Statistical parameters of the top 10 hypotheses of ALK5 kinase inhibitors generated by HypoRefine program.

Hypo no.	Total cost	Cost diff.[a]	RMSD (Å)	Correlation (r)	Features[b]
Hypo1	92.005	107.807	1.197	0.944654	$ADZZV_2$
Hypo2	92.0645	107.7975	1.2129	0.943007	$ADZZV_2$
Hypo3	92.5636	107.2984	1.26659	0.937419	$ADZRV_2$
Hypo4	94.0101	105.8519	1.32083	0.931736	$ADZRV_2$
Hypo5	98.8033	101.0587	1.43408	0.919475	$ALZZV_2$
Hypo6	100.93	98.932	1.55015	0.904635	$ADLZZV_2$
Hypo7	107.528	92.34	1.74188	0.877886	$AALZV_2$
Hypo8	110.568	89.394	1.81719	0.866309	$AAZZV_2$
Hypo9	112.106	87.756	1.86336	0.858795	AZZZ
Hypo10	112.474	87.388	1.85186	0.860787	$ADZRV_1$

[a] (Null cost-total cost), null cost = 199.862, fixed cost = 75.6445, configuration cost = 13.5555. All cost values are in bits.
[b] A, D, Z, L, and V represent hydrogen-bond acceptor, hydrogen-bond donor, hydrophobic aromatic feature, hydrophobic aliphatic moiety, and excluded volume, respectively.

2.2.2. Fischer's randomization test

Fisher's randomization test method was applied to evaluate the statistical relevance of Hypo1. The program used is CatScramble module within Catalyst. CatScramble mixes up activity values of all training set compounds to check whether there is a strong correlation between the structures and activity. The confidence level was set to 95%, so a total of 19 random spreadsheets were created for generating pharmacophore models. The results are shown in Fig. 5. From Fig. 5, we can see that the total costs of all pharmacophore models generated using the 19 random spreadsheets are much higher than the total costs of corresponding original pharmacophore models. These results provide confidence on our pharmacophore model.

2.3. Virtual screening

2.3.1. Pharmacophore model based virtual screening

The validated Hypo1 was used as a 3D structural query for retrieving potent compounds from chemical databases including Specs (135 556 molecules), NCI (238 819 molecules), MayBridge (59 652 molecules), and Chinese Nature Product Database (CNPD) (43 055 molecules), as well as an in-house chemical database. A total of 19 158 compounds were retrieved from the first screening. The hit compounds were further screened by using Lipinski's rule of five to make them more drug-like, and a total of 12 474 molecules passed this filtration. Finally 1668 compounds were selected at this stage by restricting the minimum estimated activity to 1 μM.

2.3.2. Docking study

To further refine the retrieved hits, the 1668 compounds were docked into the inhibitor binding site of ALK5 by using LigandFit within Discovery Studio 1.7 program package. 3D structure of ALK5 was taken from the crystal structure of ALK5–LY364947 complex (PDB entry: 1PY5) [27]. Since the water molecule W5 in 1PY5 has been found to be highly conserved in the reported crystal structures of ALK5–ligand complexes, and it has been thought to play some important roles in ALK5–ligand interaction [23,32], W5 was also included as a part of the receptor. LigScore1 scoring function was used as the sorting function since it performed better than others in a pre-evaluating process. The top 100 compounds were selected, and 10 of them are shown in Table S3 (see Supplementary material).

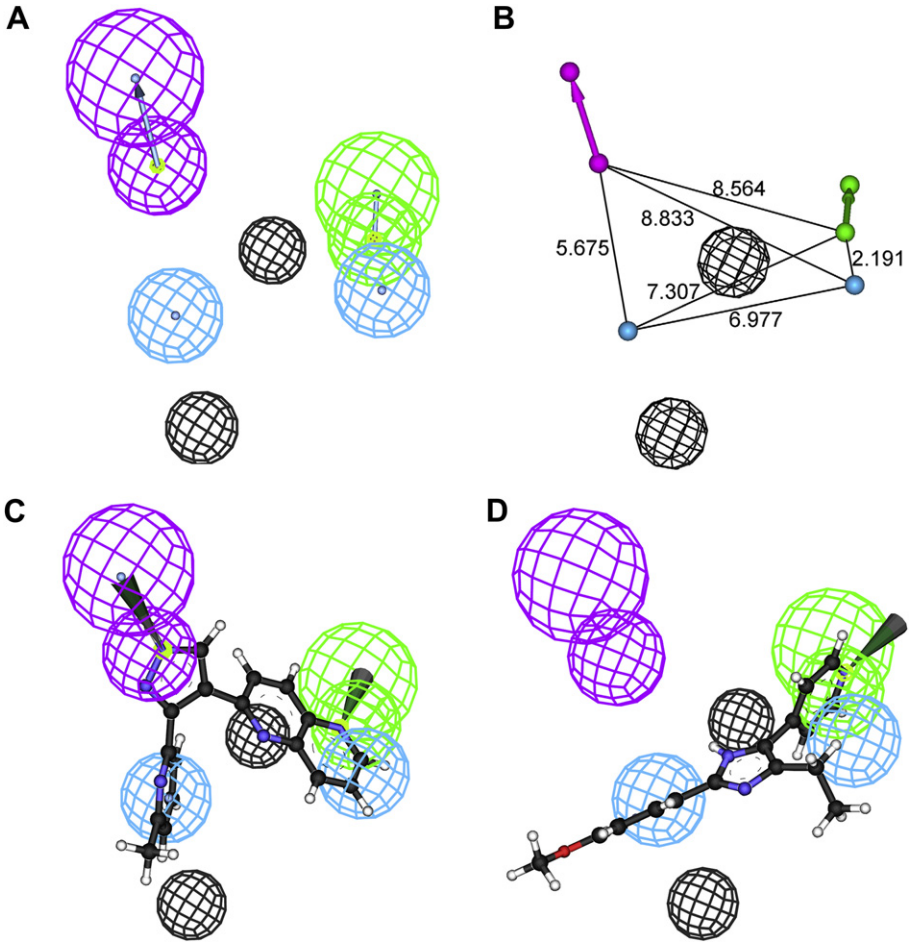

Fig. 3. Pharmacophore model of ALK5 inhibitors generated by HypoRefine. (A) The best HypoRefine pharmacophore model, Hypo1. (B) 3D spatial relationship and geometric parameters of Hypo1. (C) Hypo1 aligned with the most-active compound **1** (IC_{50}: 4 nM). (D) Hypo1 aligned with the least active compound **21** (IC_{50}: 30 000 nM). Pharmacophore features are color coded: green – hydrogen-bond acceptor, magenta – hydrogen-bond donor, blue – hydrophobic aromatic feature, black – excluded volume. (For interpretation of the references to color in this figure legend, the reader is referred to the web version of this article.)

Fig. 6 shows a possible docking model of one of the most-active compounds (compound **108**, see Table S3). One can see that compound **108** is well docked into the active site of ALK5. And three hydrogen-bond interactions are formed between compound **108** and ALK5: one is between the amino group on the triazine of compound **108** and the backbone carboxyl group of His283; one is between the pyrimidine nitrogen and the hydroxyl group of Ser280; that last one is between the other nitrogen of pyrimidine and the conserved water molecule. The first type of hydrogen-bond interactions are also usually found in other kinase–ligand complexes [34,35].

3. Discussion

In this study, we first performed a qualitative pharmacophore modeling to identify the critical common chemical features necessary for potent ALK5 inhibitors. Following the information provided by the qualitative model, a quantitative pharmacophore modeling was then carried out. The best quantitative pharmacophore model, Hypo1, consists of four features: one hydrogen-bond acceptor, one hydrogen-bond donor, and two hydrophobic aromatic features. These features together with their spatial arrangement are consistent with those of the qualitative model (see Figs. 2 and 3). In the quantitative model, two excluded volumes are also involved, which indicate that such regions in the 3D space should not be occupied by any atom for ALK5 inhibitors. Subsequently, the best quantitative pharmacophore model was further validated by test set and Fischer's randomization test method. Results obtained by the test set method show a fairly good correlation between the experimental and estimated IC_{50} values (correlation coefficient of 0.841), indicating a good predictive capacity. And results of Fischer's randomization test by using CatScramble program within Catalyst further confirmed the statistical confidence of Hypo1.

It seems that the quantitative pharmacophore model has been correctly established and well validated. However, one may still wonder whether the chemical features and their spatial arrangement described in the pharmacophore model are consistent with the actual ligand–protein interactions, since all the pharmacophore models developed here are based on the known ligands of ALK5 protein. For answering this question, one needs a crystal structure of ALK5 combined with a potent inhibitor. Fortunately the crystal structure of ALK5 in complex with compound **1**, which is the most-active compound in the training set, is available from Protein Data Bank (PDB entry: 1VJY) [25]. Thus the hypothesis Hypo1 was mapped onto the complex of ALK5–compound **1**. Again, the conserved water molecule W1001 in 1VJY, which corresponds to W5 in 1PY5, was also included. The mapping result is shown in Fig. 7. Clearly the hydrogen-bond donor feature of Hypo1 corresponds to the hydrogen-bond interaction formed between pyrazole nitrogen (hydrogen donor) and the oxygen (hydrogen acceptor) of Asp351. And the hydrogen-bond acceptor feature of Hypo1

Table 2
Experimentally measured and predicted (by Hypo1) activity for the training set compounds.

Compound	Exptl.[a]	Pred.[b]	Error[c]	Fit value[d]	Reference
1	4	1.6	−2.5	8.69	[25]
2	6	4.9	−1.2	8.20	[25]
3	10	13	+1.3	7.79	[30]
4	13	9.4	−1.4	7.91	[25]
5	18	27	+1.5	7.45	[26]
6	24	38	+1.6	7.31	[30]
7	31	61	+2	7.10	[27]
8	47	330	+7.1	6.37	[27]
9	69	270	+3.9	6.46	[29]
10	78	61	−1.3	7.10	[27]
11	94	220	+2.3	6.55	[21]
12	151	190	+1.3	6.60	[27]
13	246	240	−1	6.51	[29]
14	360	370	+1	6.32	[30]
15	460	440	−1	6.24	[21]
16	877	330	−2.6	6.36	[27]
17	1023	770	−1.3	6.00	[25]
18	3990	4800	+1.2	5.21	[23]
19	5100	680	−7.5	6.05	[21]
20	19 500	8400	−2.3	4.96	[27]
21	30 000	18 000	−1.7	4.63	[22]

[a] Exptl. = experimental activity (IC_{50} values, nM).
[b] Pred. = predicted activity (IC_{50} values, nM).
[c] + means that the estimated IC_{50} is higher than the experimental IC_{50}; − means that the estimated IC_{50} is lower than the experimental IC_{50}; a value of 1 indicates that the estimated IC_{50} is equal to the experimental IC_{50}.
[d] Fit value indicates how well the pharmacophore maps the compound.

corresponds to the hydrogen-bond interaction between 1,5-naphthyridine nitrogen (hydrogen acceptor) and backbone amine (hydrogen donor) of His283. Concerning the two hydrophobic aromatic features, one maps onto the pyridyl group, the other one maps onto one ring of 1,5-naphthyridine. Finally the excluded volumes are very close to the backbone of the protein, which is reasonable. Therefore, we can conclude here that the pharmacophore model Hypo1 developed from the small molecule inhibitors of ALK5 can also correctly reflect the interactions between ALK5 and its ligands to a great extent. This further confirms the validity of the quantitative pharmacophore model Hypo1.

Here we have to mention that our pharmacophore model Hypo1 does not include any chemical feature that corresponds to any interaction mediated by the conserved water molecule (W1001 in 1VJY), although the conserved water molecule plays some important roles in mediating the ALK5–ligand interaction. A possible explanation might be that this water molecule is present widely in ALK5–inhibitor complexes, which means that no matter what the bioactivity of inhibitor is, the conserved water molecule plays very similar roles in mediating the ALK5–ligand interaction. Therefore, it is difficult to obtain a good QSAR model if the interaction mediated by the conserved water molecule is involved.

4. Materials and methods

4.1. Pharmacophore modeling

All the pharmacophore modeling calculations were carried out by using Catalyst 4.11 software package (Accelrys, San Diego, USA). The common pharmacophore features necessary for potent ALK5 inhibitors were identified by HipHop program [36], and quantitative pharmacophore models were created by HypoRefine module [37] within Catalyst.

All compounds were built in 2D/3D Visualizer within Catalyst and minimized to the closest local minimum based on the Charmm-like force field [38]. A series of energetically reasonable conformational models which represent the flexibility of each compound were generated using CatConf program within Catalyst. We chose a maximum number of 250 conformers, the 'best conformational analysis' method, and an energy threshold of 20 kcal/mol above the global energy minimum for conformation searching.

4.2. Pharmacophore model evaluation

The quality of the developed pharmacophore models was evaluated according to Debnath [39] in terms of cost functions and other statistical parameters which were calculated by HypoRefine module during hypothesis generation. A good pharmacophore model should have a high correlation coefficient, lowest total cost and RMSD values, and the total cost should be close to the fixed cost and away from the null cost. The best pharmacophore model was further validated by test set method and Fischer's randomization test [37].

4.3. Virtual screening

The best HypoRefine pharmacophore Hypo1 was used as a 3D structural query for retrieving potent molecules from chemical databases including Specs, NCI, MayBridge and CNPD, as well as an in-house chemical database. For each molecule in the databases, 100 conformers were generated with the fast conformer generation method, allowing a maximum energy of 15 kcal/mol above that of the most stable conformation. All queries were performed using

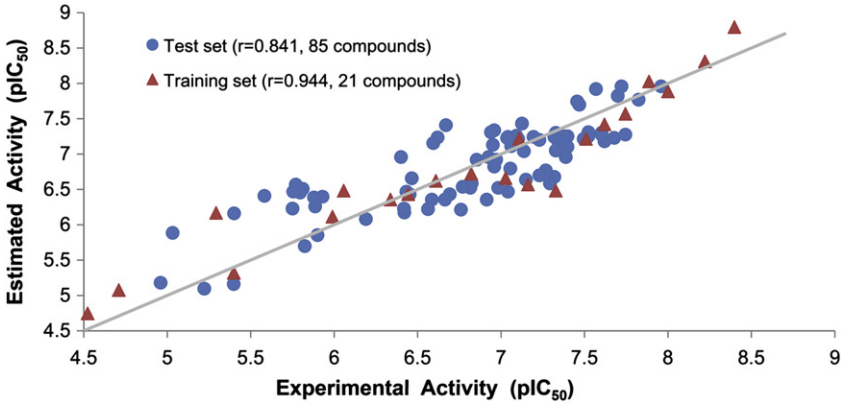

Fig. 4. Plot of the correlation (r) between the experimental activity and the predicted activity by Hypo1 for the test set molecules (in blue) and the training set molecules (in red).(For interpretation of the references to color in this figure legend, the reader is referred to the web version of this article.)

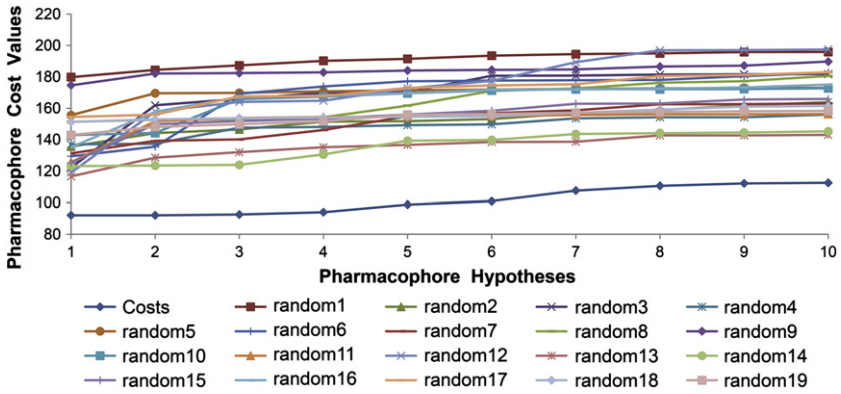

Fig. 5. The difference in total cost of hypotheses between the initial spreadsheet and 19 random spreadsheets after CatScramble run.

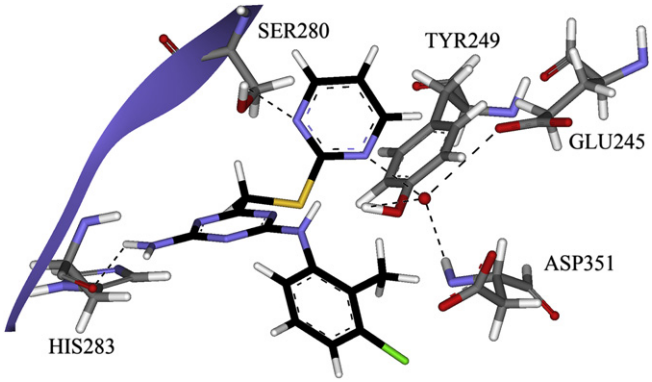

Fig. 6. A possible binding mode of compound **108** obtained from molecular docking study. The amino acid residues within the ALK5 binding site are represented in stick form. Black dotted lines represent hydrogen-bonding interactions. The red sphere represents the water molecule. (For interpretation of the references to color in this figure legend, the reader is referred to the web version of this article.)

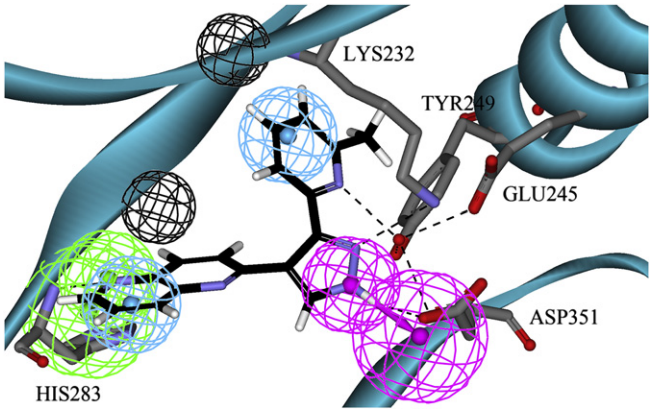

Fig. 7. Mapping of Hypo1 onto X-ray crystal structure of ALK5–compound **1**. The amino acid residues within the ALK5 binding site are represented in stick form, the backbone of the protein is represented in ribbon form. Black dotted lines represent hydrogen-bonding interactions. Pharmacophore features are color coded: green – hydrogen-bond acceptor, magenta – hydrogen-bond donor, blue – hydrophobic aromatic feature, black – excluded volume. The red sphere represents the water molecule. (For interpretation of the references to color in this figure legend, the reader is referred to the web version of this article.)

the Fast Flexible Search Databases/Spreadsheets method within the Catalyst DBServer module. The hit compounds were further filtered by Lipinski's rules to make them more drug-like.

4.4. Docking protocol

The docking study was performed with the use of LigandFit [40] program in Discovery Studio 1.7 (Accelrys, San Diego, USA). The Dreiding force field was used for all calculations. The crystal structure of ALK5 combined with LY364947 (PDB entry: 1PY5) was used as the coordinates of reference protein. Conformations of each ligand compound were created with Monte Carlo simulation (15 000 trials) and flexible fit was selected. A grid resolution was set to 0.5 Å. The RMSD threshold and score threshold were set to 2.0 Å and 20 kcal/mol, respectively. Each of the saved conformations was evaluated and ranked using the scoring functions including LigScore1, LigScore2, PLP1, PLP2, JAIN, PMF and LUDI [41]. However, a pretest result showed that the LigScore1 scoring function performed better than others. Thus LigScore1 was used as the sorting function in this work.

5. Conclusion

In this account, chemical feature based 3D pharmacophore models of ALK5 kinase inhibitors have been developed with the aid of HipHop and HypoRefine modules in Catalyst program package. The best quantitative pharmacophore model, Hypo1, was characterized by the lowest total cost value (92.055), the highest cost difference (107.807), the lowest RMSD (1.197), and the best correlation coefficient (0.944651). The fixed cost and null cost are 75.6445 and 199.862 bits, respectively. Hypo1 contains four features: one hydrogen-bond acceptor, one hydrogen-bond donor, two hydrophobic aromatic features. Two excluded volumes are also included in Hypo1. This pharmacophore model was further validated by test set and Fischer's randomization test method. Results obtained by the test set method show a fairly good correlation between the experimental and estimated IC_{50} values (correlation coefficient of 0.841), indicating a good predictive capacity. And results of Fischer's randomization test by using CatScramble program within Catalyst further confirmed the statistical confidence of Hypo1. Then the model Hypo1 was used as a 3D query to screen several databases including Specs, NCI, Maybridge, CNPD and an in-house chemical database for retrieving new potent inhibitors of ALK5. The hit compounds were subsequently subjected to filtering by Lipinski's rule of five and docking studies to refine the retrieved hits. Finally a total of 100 compounds were selected and some of them have been shifted to *in vitro* and *in vivo* studies, whose results will be reported in the near future.

Acknowledgement

This work was supported by the National Natural Science Foundation of China (30772651, 20872100) and the Youth Foundation of Sichuan Province (08ZQ026-030).

Appendix. Supplementary data

Supplementary data associated with this article can be found in the online version, at doi:10.1016/j.ejmech.2009.07.008.

References

[1] J. Plum, M. De Smedt, G. Leclercq, B. Vandekerckhove, J. Immunol. 154 (1995) 5789–5798.
[2] S.M. Wahl, J. Swisher, N. McCartney-Francis, W. Chen, J. Leukoc. Biol. 76 (2004) 15–24.
[3] D.T. Wu, M. Bitzer, W. Ju, P. Mundel, E.P. Bottinger, J. Am. Soc. Nephrol. 16 (2005) 3211–3221.
[4] R. Derynck, Y. Zhang, X.-H. Feng, Cell 95 (1998) 737–740.
[5] J.M. Yingling, K.L. Blanchard, J.S. Sawyer, Nat. Rev. Drug Discov. 3 (2004) 1011–1022.
[6] W.A. Border, N.A. Noble, N. Engl. J. Med. 331 (1994) 1286–1292.
[7] S. Kanzler, A.W. Lohse, A. Keil, J. Henninger, H.P. Dienes, P. Schirmacher, S. Rose-John, K.H. Meyer Zum Buschenfelde, M. Blessing, Am. J. Physiol. Gastrointest. Liver Physiol. 276 (1999) G1059–G1068.
[8] Y. Kanamaru, A. Nakao, M. Mamura, Y. Suzuki, I. Shirato, K. Okumura, Y. Tomino, C. Ra, J. Immunol. 166 (2001) 2818–2823.
[9] A. Bergeron, P. Soler, M. Kambouchner, P. Loiseau, B. Milleron, D. Valeyre, A.J. Hance, A. Tazi, Eur. Respir. J. 22 (2003) 69–76.
[10] C. Schramm, M. Protschka, H.H. Kohler, J. Podlech, M.J. Reddehase, P. Schirmacher, P.R. Galle, A.W. Lohse, M. Blessing, Am. J. Physiol. Gastrointest. Liver Physiol. 284 (2003) G525–G535.
[11] R.K. Gregg, R. Jain, S.J. Schoenleber, R. Divekar, J.J. Bell, H.-H. Lee, P. Yu, H. Zaghouani, J. Immunol. 173 (2004) 7308–7316.
[12] N.M. Moutsopoulos, J. Wen, S.M. Wahl, Curr. Opin. Immunol. 20 (2008) 234–240.
[13] R.B. Luwor, A.H. Kaye, H.-J. Zhu, J. Clin. Neurosci. 15 (2008) 845–855.
[14] Z. Qi, N. Atsuchi, A. Ooshima, A. Takeshita, H. Ueno, Proc. Natl. Acad. Sci. U.S.A. 96 (1999) 2345–2349.
[15] G. Karlsson, Y. Liu, J. Larsson, M.-J. Goumans, J.-S. Lee, S.S. Thorgeirsson, M. Ringner, S. Karlsson, Physiol. Genomics 21 (2005) 396–403.
[16] N.J. Laping, J.I. Everitt, K.S. Frazier, M. Burgert, M.J. Portis, C. Cadacio, L.I. Gold, C.L. Walker, Clin. Cancer Res. 13 (2007) 3087–3099.
[17] N.J. Laping, S. Huet, in: P. ten Dijke, C.-H. Heldin (Eds.), Smad Signal Transduction, Springer, The Netherlands, 2006, pp. 443–459.
[18] E. Suzuki, S. Kim, H.-K. Cheung, M.J. Corbley, X. Zhang, L. Sun, F. Shan, J. Singh, W.-C. Lee, S.M. Albelda, L.E. Ling, Cancer Res. 67 (2007) 2351–2359.
[19] K. Fu, M.J. Corbley, L. Sun, J.E. Friedman, F. Shan, J.L. Papadatos, D. Costa, F. Lutterodt, H. Sweigard, S. Bowes, M. Choi, P.A. Boriack-Sjodin, R.M. Arduini, D. Sun, M.N. Newman, X. Zhang, J.N. Mead, C.E. Chuaqui, H.-K. Cheung, X. Zhang, M. Cornebise, M.B. Carter, S. Josiah, J. Singh, W.-C. Lee, A. Gill, L.E. Ling, Arterioscler. Thromb. Vasc. Biol. 28 (2008) 665–671.
[20] M. Lahn, B. Berry, S. Kloeker, J. Yingling, in: P. ten Dijke, C.-H. Heldin (Eds.), Smad Signal Transduction, Springer, The Netherlands, 2006, pp. 415–442.
[21] J.F. Callahan, J.L. Burgess, J.A. Fornwald, L.M. Gaster, J.D. Harling, F.P. Harrington, J. Heer, C. Kwon, R. Lehr, A. Mathur, B.A. Olson, J. Weinstock, N.J. Laping, J. Med. Chem. 45 (2002) 999–1001.
[22] I. Yakymovych, U. Engstrom, S. Grimsby, C.H. Heldin, S. Souchelnytskyi, Biochemistry 41 (2002) 11000–11007.
[23] J.S. Sawyer, B.D. Anderson, D.W. Beight, R.M. Campbell, M.L. Jones, D.K. Herron, J.W. Lampe, J.R. McCowan, W.T. McMillen, N. Mort, S. Parsons, E.C.R. Smith, M. Vieth, L.C. Weir, L. Yan, F. Zhang, J.M. Yingling, J. Med. Chem. 46 (2003) 3953–3956.
[24] N. Dodic, F.J. Gellibert, Patent WO 0413135, 2004.
[25] F.O. Gellibert, J. Woolven, M.H. Fouchet, N. Mathews, H. Goodland, V. Lovegrove, A. Laroze, V.L. Nguyen, S. Sautet, R.L. Wang, C. Janson, W. Smith, G. Krysa, V. Boullay, A.C. de Gouville, S. Huet, D. Hartley, J. Med. Chem. 47 (2004) 4494–4506.
[26] H.Y. Li, Y. Wang, L. Yan, R.M. Campbell, B.D. Anderson, J.R. Wagner, J.M. Yingling, Bioorg. Med. Chem. Lett. 14 (2004) 3585–3588.
[27] J.S. Sawyer, D.W. Beight, K.S. Britt, B.D. Anderson, R.M. Campbell, T. Goodson, D.K. Herron, H.Y. Li, W.T. McMillen, N. Mort, S. Parsons, E.C.R. Smith, J.R. Wagner, L. Yan, F.M. Zhang, J.M. Yingling, Bioorg. Med. Chem. Lett. 14 (2004) 3581–3584.
[28] F. Gellibert, A.C. de Gouville, J. Woolven, N. Mathews, V.L. Nguyen, C. Bertho-Ruault, A. Patikis, E.T. Grygielko, N.J. Laping, S. Huet, J. Med. Chem. 49 (2006) 2210–2221.
[29] H.Y. Li, Y. Wang, C.R. Heap, C.H.R. King, S.R. Mundla, M. Voss, D.K. Clawson, L. Yan, R.M. Campbell, B.D. Anderson, J.R. Wagner, K. Britt, K.X. Lu, W.T. McMillen, J.M. Yingling, J. Med. Chem. 49 (2006) 2138–2142.
[30] D.K. Kim, Y. Jang, H.S. Lee, H.J. Park, J. Yoo, J. Med. Chem. 50 (2007) 3143–3147.
[31] C.A. Lipinski, J. Pharmacol. Toxicol. Methods 44 (2000) 235–249.
[32] J. Singh, C.E. Chuaqui, P.A. Boriack-Sjodin, W.C. Lee, T. Pontz, M.J. Corbley, H.K. Cheung, R.M. Arduini, J.N. Mead, M.N. Newman, J.L. Papadatos, S. Bowes, S. Josiah, L.E. Ling, Bioorg. Med. Chem. Lett. 13 (2003) 4355–4359.
[33] H.Y. Wang, Z.X. Cao, L.L. Li, P.D. Jiang, Y.L. Zhao, S.D. Luo, L. Yang, Y.Q. Wei, S.Y. Yang, Bioorg. Med. Chem. Lett. 18 (2008) 4972–4977.
[34] G. Xu, L.L. Searle, T.V. Hughes, A.K. Beck, P.J. Connolly, M.C. Abad, M.P. Neeper, G.T. Struble, B.A. Springer, S.L. Emanuel, R.H. Gruninger, N. Pandey, M. Adams, S. Moreno-Mazza, A.R. Fuentes-Pesquera, S.A. Middleton, L.M. Greenberger, Bioorg. Med. Chem. Lett. 18 (2008) 3495–3499.
[35] J. Zou, H.-Z. Xie, S.-Y. Yang, J.-J. Chen, J.-X. Ren, Y.-Q. Wei, J. Mol. Graph. Model. 27 (2008) 430–438.
[36] H. Yu, Z. Wang, L. Zhang, J. Zhang, Q. Huang, Chem. Biol. Drug Des. 69 (2007) 204–211.
[37] I.L. Lu, K.-C. Tsai, Y.-K. Chiang, W.-T. Jiaang, S.-H. Wu, N. Mahindroo, C.-H. Chien, S.-J. Lee, X. Chen, Y.-S. Chao, S.-Y. Wu, Eur. J. Med. Chem. 43 (2008) 1603–1611.
[38] B.R. Brooks, R.E. Bruccoleri, B.D. Olafson, D.J. States, S. Swaminathan, M. Karplus, J. Comput. Chem. 4 (1983) 187–217.
[39] A.K. Debnath, J. Med. Chem. 45 (2002) 41–53.
[40] C.M. Venkatachalam, X. Jiang, T. Oldfield, M. Waldman, J. Mol. Graph. Model. 21 (2003) 289–307.
[41] X.Q. Deng, H.Y. Wang, Y.L. Zhao, M.L. Xiang, P.D. Jiang, Z.X. Cao, Y.Z. Zheng, S.D. Luo, L.T. Yu, Y.Q. Wei, S.Y. Yang, Chem. Biol. Drug Des. 71 (2008) 533–539.